scientific reports

Check for updates

OPEN

The relationship between regional homogeneity in resting-state functional magnetic resonance imaging and cognitive function in depressive disorders with migraine

Wensheng Chen[1,2], Guojun Xie[1,2], Caixia Xu[1], Jiaquan Liang[1]✉ & Chunguo Zhang[1]✉

Patients with depressive disorder with migraine (DDWM) are common, yet the neural mechanisms and brain function changes associated with this comorbidity remain partially understood. This study explores regional homogeneity (ReHo) abnormalities in resting-state functional magnetic resonance imaging (fMRI) and cognitive function in DDWM patients. We recruited 29 patients with DDWM, 34 patients with depressive disorder without migraine (DDWOM), and 43 matched healthy controls (HC). All participants underwent rs-fMRI scans, and imaging data were analyzed using ReHo. Cognitive function was assessed with the Repeatable Battery for the Assessment of Neuropsychological Status. We also employed support vector machine (SVM) analysis to evaluate whether abnormal ReHo values could distinguish DDWM. he DDWM group exhibited significantly lower ReHo values in the left cuneus and left calcarine compared to the DDWOM group. ReHo values in these regions were negatively correlated with pain scores on the Visual Analogue Scale ($r = -0.3628$, $p = 0.0001$; $r = -0.3142$, $p = 0.001$) and positively correlated with the List_Recall score on RBANS ($r = 0.260$, $p = 0.007$). SVM analysis indicated that the left cuneus ReHo value could distinguish DDWM from DDWOM with 78.09% accuracy, 87.66% sensitivity, and 74.33% specificity. The left cuneus and left calcarine are potential biomarkers for migraine symptoms in DDWM, with the left cuneus affecting cognitive function related to memory.

Keywords Depressive disorder with migraine, Resting-state functional magnetic resonance imaging, Regional homogeneity, Repeatable battery for the assessment of neuropsychological status, Support vector machine

Depressive disorder is a mental illness marked by persistent low mood, sleep disturbances, cognitive decline, and vegetative symptoms. It has a lifetime prevalence of around 20%[1]. In recent years, depression has become one of the leading causes of the global disease burden[2]. Comorbidity rates in depressive disorders are high, with migraine being the most common. Patients with depression are three times more likely to experience migraines than the general population, while those with migraines are five times more likely to develop depression[3]. Patients with depressive disorder with migraine (DDWM) often have a poor prognosis[4], exhibiting more severe headache-related symptoms, a higher risk of chronic migraine, and a more severe clinical course.

Current research on the mechanisms of DDWM suggests that it is related to both environmental and genetic factors[5,6]. A study involving 1,000 pairs of female twins, both monozygotic and dizygotic, found a 20% prevalence of migraine and a 23% prevalence of depression. The heritability of depression was estimated at 58%, while that of migraine was approximately 44%[5]. A meta-analysis of 12 studies by Antonaci et al. reported that the prevalence of DDWM ranged from 8.6 to 47.9%[7]. DDWM is a significant risk factor for chronic migraine, medication overuse, treatment resistance, increased migraine-related disability, emotional dysregulation, and suicidal behavior, all of which contribute to substantial impairments in quality of life and psychosocial functioning[8–11]. Patients with DDWM typically experience more severe depressive symptoms, a higher suicide risk, and poorer treatment outcomes. Therefore, it is critical to prioritize the prevention, identification, and

[1]Department of Psychiatry, The Third People's Hospital of Foshan, Foshan 528000, Guangdong, China. [2]Wensheng Chen and Guojun Xie contributed equally to this work. ✉email: 417891714@qq.com; cgzhang1994@163.com

treatment of this comorbidity. Further research into the mechanisms of DDWM is essential to enhance clinical diagnosis and treatment strategies.

Regional Homogeneity (ReHo) analysis in resting-state functional magnetic resonance imaging (rs-fMRI) is a commonly used method that measures the synchrony of time-series signals between a given voxel and its neighboring voxels, calculated using the Kendall's coefficient of concordance (KCC)[12]. Changes in ReHo values, whether increased or decreased, indicate abnormal neural activity, reflecting disruptions in the synchrony of local neural activity[13]. ReHo can also evaluate the severity of emotional symptoms and has high test-retest reliability[13,14]. ReHo analysis has been widely applied to the study of various neuropsychiatric disorders, such as mild cognitive impairment, depression, schizophrenia, and bipolar disorder (BD), offering valuable insights into the neural mechanisms underlying these conditions[13,15–18]. Additionally, ReHo is considered a promising method for distinguishing between different mood disorders, even differentiating subthreshold BD from major depressive disorder (MDD). A study on drug-naïve BD and unipolar disorder (UD) patients found that abnormal ReHo in the thalamus could effectively differentiate these two conditions[19].

The brain of DDWM patients differ from those of individuals with isolated migraine or depressive disorder. Numerous neuroimaging studies on migraine have identified functional changes in specific brain regions, suggesting that these abnormalities may be linked to depressive symptoms in migraine without aura[20–22]. Numerous neuroimaging studies on migraine have investigated changes in brain activity, pinpointed dysfunctional regions, and hypothesized that these areas could play a role in the manifestation of depressive symptoms in individuals with migraine without aura[20,21,23]. A prior study discovered that both migraine and depression together influenced the development of the left mPFC, potentially contributing to the shared symptoms observed in both conditions[24]. We hypothesize that migraine and depressive disorder influence brain states differently, particularly in regions associated with clinical symptoms and shared etiological risk factors for migraine-depression comorbidity. To our knowledge, few studies have used ReHo analysis to compare the differences between DDWM and DDWOM.

Support vector machine (SVM) is a specialized type of supervised machine learning, utilizing multivariable pattern recognition techniques, which are employed to predict psychosis based on neuroanatomical markers[25]. SVM can efficiently extract relevant information and features from various brain regions, which are then utilized to categorize patients and healthy controls (HC) based on neuroimaging data, such as MRI data[26], thereby enhancing the robustness of the classification outcomes. SVM technology has been widely applied in research on depression[27].

In this study, we performed ReHo analysis to compare differences between DDWM, DDWOM, and HC groups. We hypothesize that: (1) abnormal ReHo in the brain will be observed in DDWM patients; (2) these ReHo abnormalities may be related to the clinical features of the patients; (3) support vector machine (SVM) methods will be used to explore whether abnormal ReHo values can be used to identify DDWM.

Subjects and methods

Subjects

The study included inpatients from the Third People's Hospital of Foshan (Foshan Mental Health Center) between July 2020 and September 2022, aged 17 to 59 years, with no gender restrictions. Participants were required to have at least a primary school education. A total of 106 individuals were recruited, including 29 with DDWM, 34 with DDWOM, and 43 healthy controls (HC). All participants provided informed consent before participating in the study.

Depression was diagnosed according to the criteria in the Diagnostic and Statistical Manual of Mental Disorders, Fifth Edition (DSM-5)[28]. The diagnostic criteria for migraine without aura were based on the International Classification of Headache Disorders, Third Edition (beta version, ICHD-3 beta)[29].

The Visual Analogue Scale (VAS) was used to assess pain, with scores ranging from 1 to 10: 1–3 points indicating mild pain, 4–6 points indicating moderate pain, and 7–10 points indicating severe pain. DDWM or DDWOM diagnosis was confirmed through clinical interviews conducted by two or more qualified psychiatrists. The DDWM group was diagnosed with depression and migraine without aura based on DSM-5 and ICHD-3 beta criteria, a total score ≥ 17 on the 24-item Hamilton Rating Scale for Depression (HRSD-24), and no prior use of antidepressants or migraine prevention medication. Migraine patients had no headache attacks at least 3 days prior to the fMRI examination and were followed up 3 days after scanning to confirm they remained headache-free, ensuring no interference with functional imaging results.

The DDWOM group was diagnosed with depression according to DSM-5 criteria and confirmed by two qualified psychiatrists, with a total HRSD-24 score ≥ 17 and currently in a depressive episode, without a history of migraine or other types of headaches. The healthy control group consisted of 43 healthy individuals matched for age and gender with the patient groups, recruited through posters. All controls were screened by professionals using the DSM-IV-TR Axis I Disorders-Patient Edition structured clinical interview to confirm the absence of psychiatric disorders.

Exclusion criteria included: (1) current pregnancy or breastfeeding; (2) alcohol or drug abuse; (3) coexisting major medical or neurological conditions; (4) MRI contraindications, such as claustrophobia. This study was conducted following the principles of the Declaration of Helsinki and was approved by the Ethics Committee of the Third People's Hospital of Foshan (Foshan Mental Health Center) (Ethics Approval Number: FSSY-LS202109).

Procedure

Clinical symptom assessment was conducted through interviews to gather basic demographic information (age, gender, and education level) and detailed information about the patients' condition, including age of onset and

family history, with assistance from nursing staff. The Oldfield Handedness Questionnaire was used to determine handedness, ensuring that all participants were right-handed.

The Hamilton Rating Scale for Depression-24 (HRSD-24) was used to assess depressive symptoms in all participants. Cognitive function was evaluated using the Repeatable Battery for the Assessment of Neuropsychological Status (RBANS), a cognitive testing tool developed by Randolph in 1998. RBANS is widely used to assess cognitive function in patients with psychiatric and neurological disorders. It includes five cognitive domains (with ten subtests), including Immediate Memory (Story Memory and List Learning), Visuospatial/Constructional, Language, Attention, and Delayed Memory. RBANS is known for its simplicity, high sensitivity, short administration time, and effectiveness, making it highly suitable for repeated assessments[30].

Imaging data acquisition and preprocessing

The rs-fMRI data for the three groups of subjects were acquired using a GE Signa Pioneer 3.0T MRI scanner at the Third People's Hospital of Foshan (Foshan Mental Health Center). During the scan, participants were required to lie still, relax, keep their eyes closed, refrain from external activities, minimize cognitive activities, and remain awake throughout the procedure.

The scanning parameters were as follows:

1. T1 Structural Imaging: Scan duration was 338 s (5 min 38 s), with a repetition time (TR) of 8.6 ms, echo time (TE) of 3.3 ms, inversion time (TI) of 450 ms, flip angle of 12°, matrix size of 256 × 256, slice thickness of 1 mm, and a total of 172 slices.
2. BOLD Functional Imaging: Resting-state data were acquired using the gradient echo-single shot-echo planar imaging (GRE-SS-EPI) sequence with the following parameters: TR/TE = 2000/30 ms, flip angle of 90°, field of view (FOV) of 240 mm × 240 mm, matrix of 64 × 64, slice thickness of 4 mm, 36 slices, slice gap of 1 mm, and a total of 250 volumes.

Image data preprocessing was performed using DPABI_V6.1 (http://rfmri.org/dpabi) on the Matlab 2018b platform, with the following steps:

1. Convert DICOM data to NIFTI format;
2. Discard the first 10 time points, and perform slice timing correction and head motion correction (data with head motion exceeding 2.0 mm translation or 2.0° rotation were excluded);
3. Spatial normalization (resampling to 3 mm × 3 mm × 3 mm) to the standard Montreal Neurological Institute (MNI) template;
4. Remove linear drift;
5. Regress out cerebrospinal fluid and white matter signals, global mean signal, and Friston 24 head motion parameters to reduce confounding factors and improve result accuracy;
6. Apply band-pass filtering (0.01–0.08 Hz) and detrending to reduce low-frequency drift, high-frequency respiratory and cardiac noise.

ReHo values were calculated based on Kendall's coefficient of concordance (KCC). The ReHo value for each voxel was computed using a cluster of 27 voxels, resulting in an ReHo map for each voxel. Each voxel's ReHo value was then divided by the global mean ReHo value, followed by Fisher Z transformation for normalization. Finally, Gaussian smoothing (FWHM, 4 mm × 4 mm × 4 mm) was applied to obtain the brain ReHo images. All processing was conducted directly using DPARSF software to obtain zReHo images.

Statistical analysis

Data analysis was conducted using SPSS 20.0 software (SPSS Inc., Chicago, Illinois, USA), with variance analysis and chi-square tests used to compare demographic and clinical variables between different groups. Post-hoc comparisons were adjusted using LSD or Tamhane corrections based on variance homogeneity, with a significance level set at $p < 0.05$.

The rs-fMRI data were analyzed using the DPARSF tool for one-way ANOVA and two-sample t-tests, with Gaussian random field (GRF) theory applied for correction. Age, gender, and head motion parameters were included as covariates to explore whole-brain ReHo differences between DDWM patients, DDWOM patients, and HC. The DPARSF tool provided specific anatomical locations and corresponding results.

Subsequently, age, gender, and education level of the subjects were used as covariates to extract significant ReHo values from brain regions with differences, and partial correlation analyses were performed with RBANS scores, with P-values corrected using Bonferroni adjustments.

SVM analysis

SVM is a widely used algorithm for classification and regression problems[31]. In this study, SVM analysis was conducted using the MVPANI tool[32] on the Matlab 2018 platform to determine whether abnormal ReHo values can effectively differentiate between DDWM and DDWOM. MVPANI employs a simple graphical user interface to input ReHo image files (.nii) for both DDWM and DDWOM groups, and an Excel file (.xlsx) was created to provide labels. The ReHo images were used directly for MVPA analysis without additional feature preprocessing. All voxels within the whole-brain mask were utilized without feature selection. The classification algorithm used was C-SVC with default parameters (linear kernel; penalty coefficient C = 1). The method involved 5000 permutation tests with ten-fold cross-validation. The output included classification accuracy (with both specificity and sensitivity), ROC curves, and average weight maps.

Variables	DDWM (Mean ± SD, $n = 29$)	DDWOM (Mean ± SD, $n = 34$)	HC (Mean ± SD, $n = 43$)	F/χ^2	p
Sex (male/female)	29(19/10)	34(20/14)	43(24/19)	3.774	0.052[a]
Age (years)	30.6 ± 11.8	27.1 ± 10.9	34.4 ± 11.9	2.53	0.115[b]
Years of education (years)	12.2 (2.49)	11.9 (2.38)	13.0 (3.76)	2.957	0.228[b]
HRSD-24	25.3 ± 6.63	21.77 ± 6.70	2.50 ± 3.36	75.149	<0.01[b]
VAS	4.45(1.68)	0(0)	0(0)	101.744	<0.01[b]

Table 1. Demography and clinical characteristics. DDWM refers to depressive disorder with migraine; DDWOM refers to depressive disorder without migraine; HC stands for healthy control; HDRS-24 is the Hamilton depression rating scale-24. a indicates the *P* value from the chi-square test. b indicates the *P* value from the analysis of variance.

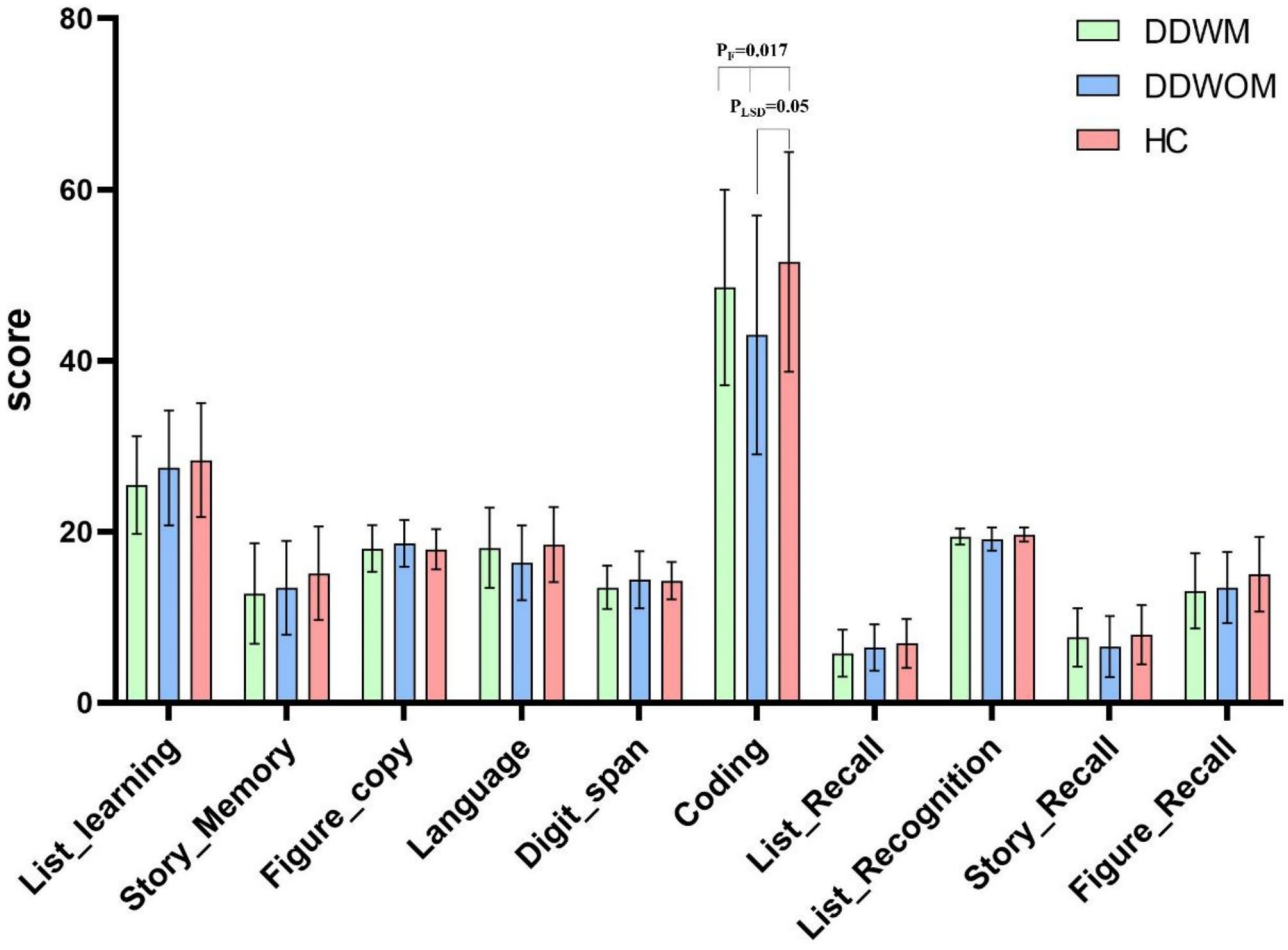

Fig. 1. compares the RBANS scores among the three groups. There is a difference in attention (symbol coding) between DDWOM and HC.

Results

Demographic and clinical characteristics

The study included 106 participants, and imaging data collection was completed. Among them, there were 29 DDWM patients, 34 DDWOM patients, and 43 HC controls. The results indicated that there were no significant differences in gender, age, and education level among the three groups ($p > 0.05$). However, there were significant differences in HDRS-24 and VAS scores ($p < 0.05$), with both DDWM and DDWOM groups showing higher HDRS-24 scores compared to HC (see Table 1). An analysis of variance (ANOVA) of RBANS scores revealed significant differences in attention (symbol coding) scores ($p = 0.017$). LSD multiple comparisons indicated a significant difference between the DDWOM and HC groups ($p = 0.005$), as shown in Fig. 1.

	Cluster location	Peak (MNI)			Number of voxels	T value	F	*p*
		x	y	z				
ANOVA	Left Cuneus	− 3	− 87	30	15	17.04	11.47	< 0.05
	Left Calcarine	− 21	− 66	9	15	21.86	11.47	< 0.05
DDWM vs. DDWOM	Left Cuneus	0	− 84	30	43	− 5.22	–	< 0.05
	Left Calcarine	− 18	− 66	9	20	− 4.01	–	< 0.05

Table 2. Differences in ReHo brain regions among the DDWM, DDWOM, and HC groups.

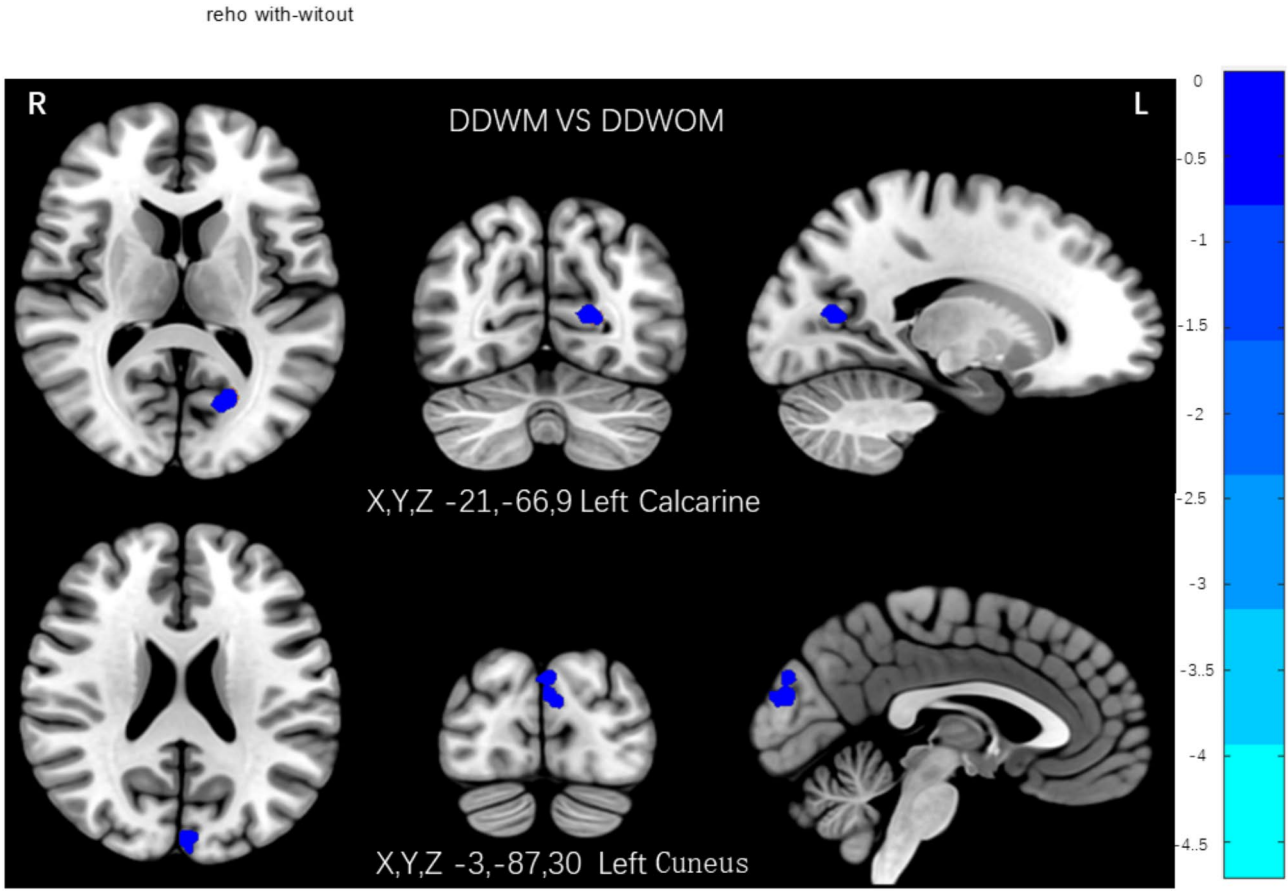

Fig. 2. Abnormal brain regions in the DDWM group vs. the DDWOM group. L represents the left side, and R represents the right side; blue indicates brain regions where the ReHo values are lower in the DDWM group compared to the DDWOM group. GRF correction was applied, with voxel-level $P < 0.001$ and cluster-level $P < 0.05$.

ReHo value analysis

The analysis of variance for ReHo values among the three groups revealed differences in the Left Cuneus and Left Calcarine regions. Post-hoc two-sample T-tests indicated that there were no significant differences between the DDWOM group and HC group, but abnormalities were found between the DDWOM and DDWM groups. Compared to the DDWOM group, the DDWM group showed decreased ReHo values in the Left Cuneus and Left Calcarine ($p < 0.05$, GRF corrected), as shown in Table 2; Fig. 2.

In the DDWM group, the ReHo values of brain regions with differences from the DDWOM group were correlated with clinical symptoms after controlling for gender, age, and education level. The ReHo values in the Left Cuneus and Left Calcarine were negatively correlated with VAS scores ($r = -0.314$, $p = 0.001$; $r = -0.362$, $p = 0.001$). Additionally, the ReHo value in the Left Cuneus was positively correlated with the List_Recall score on the RBANS scale ($r = 0.260$, $p = 0.0071$), as shown in Fig. 3.

Results of the SVM

The regions with significant differences between the two groups, namely the Left Cuneus and Left Calcarine ReHo values, were used as input data. The output from the MVPANI tool included classification accuracy

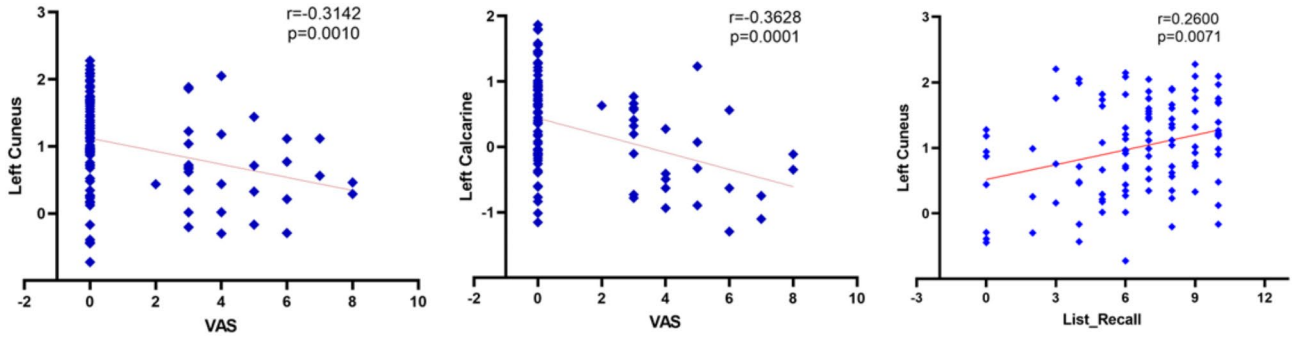

Fig. 3. Partial correlation analysis of ReHo values in the Left Cuneus and Left Calcarine with VAS and RBANS scores, with *P* values adjusted using the Bonferroni correction.

Cluster location	Accuracy (%)	Sensitivity (%)	Specificity (%)	AUC
Left Cuneus	78	74	87	0.818
Left Calcarine	66	65	68	0.744

Table 3. Classification model SVM metrics and AUC values based on ReHo values of the different brain regions.

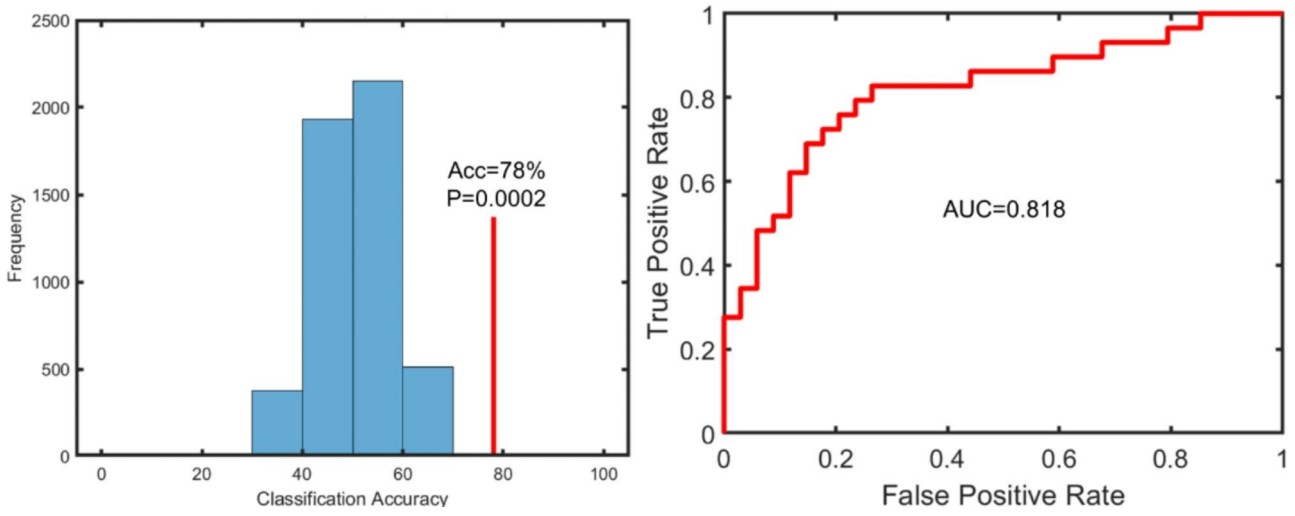

Fig. 4. The left panel shows the results of the SVM permutation test for ReHo values in the Left Cuneus, with $P < 0.05$ and 5000 permutations. The blue and red lines represent the accuracy of the permutation results and the true labels, respectively. The right panel displays the ROC curve for the SVM results of the Left Cuneus.

(with both specificity and sensitivity), ROC curves, and average weight maps. The results showed that the ROC curve area for Left Calcarine was 0.744, with an accuracy of 66%, sensitivity of 65%, and specificity of 68% in distinguishing between DDWM and DDWOM groups, but it did not pass the 5000 permutation tests ($p = 0.0778$). In contrast, the Left Cuneus ReHo values demonstrated the best recognition performance, with an ROC curve area of 0.818, accuracy of 78%, sensitivity of 74%, and specificity of 87%. This result passed the 5000 permutation tests ($p = 0.0002$), as shown in Table 3; Fig. 4.

Discussion

In this study, we found that the severity of depressive symptoms in DDWM patients was greater than in DDWOM patients, consistent with previous research. Significant differences in ReHo values among the three groups were primarily observed in the occipital lobe regions. Compared to DDWOM patients, DDWM patients showed reduced ReHo in the Left Cuneus and Left Calcarine. ReHo values in these regions were correlated with VAS and RBANS scores. Notably, Left Cuneus demonstrated the highest AUC, accuracy, sensitivity, and specificity, suggesting it may be a useful indicator for distinguishing DDWM.

Previous studies have identified brain function changes in patients with comorbid migraine and depression, particularly in areas such as the right paracentral lobule, Left Calcarine, and the left dorsolateral prefrontal cortex[33]. Both depression and migraine appear to affect the development of the left medial prefrontal cortex, potentially clarifying the common symptoms of these conditions[24]. Our study found ReHo abnormalities in the Left Calcarine, consistent with previous research. However, we did not observe abnormalities in the other regions mentioned, which may be due to factors such as the selection of research subjects, sample size, and data analysis methods. Notably, significant differences in ReHo values among the DDWM, DDWOM, and HC groups were primarily observed in the occipital lobe region.

The occipital lobe is primarily responsible for processing visual information, and damage to this area may result in declines in visual-related cognitive tasks. High-resolution MRI mapping data indicate that, compared to healthy controls, patients with depression show reduced myelin in the occipital lobe cortex[34]. Although visual impairments are not core symptoms of depression, studies[35,36] have found that depressive patients without eye diseases experience reduced visual function compared to normal individuals. Previous research has shown that depression is associated with reduced ReHo values in the left occipital middle gyrus[37], as well as decreases in the ReHo values of the lingual gyrus and precuneus[38]. Another study on ReHo in depression found that the precuneus, as part of the default mode network (DMN), had higher ReHo values compared to the normal population[39]. Additionally, the occipital cortex may be related to the symptoms of melancholic depression[40]. Many studies have also reported abnormal brain structure and functional changes in the occipital lobe of depression patients[41,42]. These findings suggest a strong association between the occipital lobe and the clinical symptoms of depression.

The cuneus, a part of the occipital lobe, lies between the visual and sensory-motor areas. The anterior-medial regions of the cuneus play a key role in processing temporal and spatial information, interacting with the lowest levels of the cortical hierarchy before engaging with other visual response areas[43]. Both the cuneus and precuneus are involved in visual information processing and are among the first regions to respond in the occipital lobe[44]. The cuneus is closely associated with depressive symptoms and serves as a neuroimaging marker for both bipolar and unipolar depression[45]. Another study observed cortical thinning in the left hemisphere (including the precuneus and cuneus) even in subjects with high familial risk for severe depression[46]. During the early stages of emotional processing (0–100 ms), reduced functional connectivity (FC) between the left parahippocampal gyrus and the left cuneus was observed[47]. The cuneus integrates somatosensory information with other sensory stimuli and supports cognitive functions such as attention, learning, and memory[48]. It, along with the fusiform gyrus, plays a key role in multisensory integration and cognitive processing, particularly in the retrieval of impact perception transmitted by Aδ fibers[49]. Ter et al. found that electrical stimulation-induced pain perception activates multiple brain regions, including the left fusiform cortex, hippocampus, primary and associative visual cortices, and extending into the cuneus and precuneus, as well as more anterior networks. These areas are part of dopaminergic pathways and negatively correlate with pain intensity ratings[50]. This finding is consistent with our observation that the ReHo values in the cuneus are negatively correlated with pain intensity ratings. The cuneus is involved in high-level cognitive functions, such as awareness, multisensory integration, and contextual memory, and plays a role in bottom-up control of visual spatial attention. These functions suggest that the cuneus interacts with default mode networks and limbic regions to maintain alertness, attention, motivation, and arousal. Thus, the cuneus plays a crucial role in visual, sensory, and cognitive processes.

Zhang et al. found reduced dALFF values in the calcarine and lingual gyri of patients with schizophrenia and MDD[51]. Elderly depressed patients with olfactory recognition impairments exhibited increased FC between the left calcarine gyrus and the left orbital frontal cortex[52]. In first-episode and treatment-naive MDD patients, significant reductions in ReHo values were observed in the right calcarine cortex both before and after transcranial auricular vagus nerve stimulation[53]. Previous studies have suggested that abnormalities in the calcarine region may impair cognitive control in depressed patients by affecting visual processing and attention[54]. Changes in brain activity in this region may be related to working memory deficits and could be associated with cognitive processes in depression. However, our results did not find a significant correlation between the Left Calcarine and cognitive functions, which may be due to differences in sample size and statistical methods.

The innovation of this study lies in combining the ReHo method from rs-fMRI with the SVM approach. After identifying brain regions with changes using the ReHo method, we further explored these findings using the SVM method. This integration facilitates a more effective search for biomarkers of DDWM.

This study has several limitations. First, due to constraints, the sample size was relatively small, which may have introduced some data variability. Future research should aim to increase the sample size to enhance the accuracy of the findings. Second, migraine patients without depressive disorders were not included, so expanding the scope to include this group in future studies would allow for a more comprehensive investigation. Finally, as a cross-sectional study, the ability to interpret the relationship between abnormal ReHo values, disease progression, and treatment effects is limited. Future research should include longitudinal follow-ups with participants to observe changes over time and explore the effects of different treatment methods.

Conclusion

In summary, our study found that the ReHo values of the Left Cuneus and Left Calcarine in the DDWM group were lower than those in the DDWOM group, indicating that the occipital lobe activity in the DDWM group is suppressed, which may be related to migraine symptoms. However, no significant differences were observed when compared to the normal group, suggesting that the role of the occipital lobe in regulating comorbid depression with migraine is unique, rather than a simple overlay of migraine and depression. The ReHo values of the Left Cuneus and Left Calcarine were negatively correlated with VAS scores, while the ReHo value of the Left Cuneus was positively correlated with the List_Recall score on the RBANS scale. SVM analysis revealed that the Left Cuneus had the optimal AUC value, accuracy, sensitivity, and specificity, which may provide a clue for

identifying DDWM. These findings of abnormal brain regions offer important insights into the neurobiological mechanisms underlying depression comorbid with migraine and provide new targets for future diagnostic and therapeutic strategies.

Data availability

The datasets used and/or analyzed during this study are available from the corresponding author (Zhang C) upon reasonable request.

Received: 17 November 2024; Accepted: 1 April 2025
Published online: 07 April 2025

References

1. Frankish, H., Boyce, N. & Horton, R. Mental health for all: A global goal. *Lancet* **392**, 1493–1494. https://doi.org/10.1016/s0140-6736(18)32271-2 (2018).
2. Simon, G. E., Moise, N. & Mohr, D. C. Management of depression in adults: A review. *Jama* **332**, 141–152. https://doi.org/10.1001/jama.2024.5756 (2024).
3. Ligthart, L. et al. Genetic risk score analysis indicates migraine with and without comorbid depression are genetically different disorders. *Hum. Genet.* **133**, 173–186. https://doi.org/10.1007/s00439-013-1370-8 (2014).
4. Lu, S. R., Fuh, J. L., Juang, K. D. & Wang, S. J. Repetitive intravenous prochlorperazine treatment of patients with refractory chronic daily headache. *Headache* **40**, 724–729. https://doi.org/10.1046/j.1526-4610.2000.00126.x (2000).
5. Yang, Y. et al. Familial aggregation of migraine and depression: insights from a large Australian twin sample. *Twin Res. Hum. Genetics: Official J. Int. Soc. Twin Stud.* **19**, 312–321. https://doi.org/10.1017/thg.2016.43 (2016).
6. Lamers, F. et al. Familial aggregation and heritability of the melancholic and atypical subtypes of depression. *J. Affect. Disord.* **204**, 241–246. https://doi.org/10.1016/j.jad.2016.06.040 (2016).
7. Antonaci, F. et al. Migraine and psychiatric comorbidity: A review of clinical findings. *J. Headache Pain* **12**, 115–125. https://doi.org/10.1007/s10194-010-0282-4 (2011).
8. Ashina, S. et al. Depression and risk of transformation of episodic to chronic migraine. *J. Headache Pain.* **13**, 615–624. https://doi.org/10.1007/s10194-012-0479-9 (2012).
9. Peck, K. R., Smitherman, T. A. & Baskin, S. M. Traditional and alternative treatments for depression: implications for migraine management. *Headache* **55**, 351–355. https://doi.org/10.1111/head.12521 (2015).
10. Radat, F. et al. Psychiatric comorbidity in the evolution from migraine to medication overuse headache. *Cephalalgia: Int. J. Headache* **25**, 519–522. https://doi.org/10.1111/j.1468-2982.2005.00910.x (2005).
11. Serafini, G. et al. Gene variants with suicidal risk in a sample of subjects with chronic migraine and affective temperamental dysregulation. *Eur. Rev. Med. Pharmacol. Sci.* **16**, 1389–1398 (2012).
12. Paulus, M. P. et al. Behavioral and functional neuroimaging evidence for prefrontal dysfunction in methamphetamine-dependent subjects. *Neuropsychopharmacol.: Off. Publ. Am. Coll. Neuropsychopharmacol.* **26**, 53–63. https://doi.org/10.1016/s0893-133x(01)00334-7 (2002).
13. Lai, C. H. & Wu, Y. T. The alterations in regional homogeneity of parieto-cingulate and temporo-cerebellum regions of first-episode medication-naïve depression patients. *Brain Imaging Behav.* **10**, 187–194. https://doi.org/10.1007/s11682-015-9381-9 (2016).
14. Zuo, X. N. & Xing, X. X. Test-retest reliabilities of resting-state FMRI measurements in human brain functional connectomics: A systems neuroscience perspective. *Neurosci. Biobehav. Rev.* **45**, 100–118. https://doi.org/10.1016/j.neubiorev.2014.05.009 (2014).
15. Liu, X. et al. Disrupted regional spontaneous neural activity in mild cognitive impairment patients with depressive symptoms: A resting-state fMRI study. *Neural Plast.* **2019** (2981764). https://doi.org/10.1155/2019/2981764 (2019).
16. Gao, W. et al. Alterations of regional homogeneity in pediatric bipolar depression: A resting-state fMRI study. *BMC Psychiatry* **14**, 222. https://doi.org/10.1186/s12888-014-0222-y (2014).
17. Guo, W. B. et al. Abnormal neural activities in first-episode, treatment-naïve, short-illness-duration, and treatment-response patients with major depressive disorder: a resting-state fMRI study. *J. Affect. Disord.* **135**, 326–331. https://doi.org/10.1016/j.jad.2011.06.048 (2011).
18. Li, H. J. et al. Surface-based regional homogeneity in first-episode, drug-naïve major depression: A resting-state FMRI study. *Biomed. Res. Int.* 374828 (2014). (2014). https://doi.org/10.1155/2014/374828
19. Liang, M. J. et al. Identify changes of brain regional homogeneity in bipolar disorder and unipolar depression using resting-state FMRI. *PLoS One* **8**, e79999. https://doi.org/10.1371/journal.pone.0079999 (2013).
20. Li, X. L. et al. A diffusion tensor magnetic resonance imaging study of corpus callosum from adult patients with migraine complicated with depressive/anxious disorder. *Headache* **51**, 237–245. https://doi.org/10.1111/j.1526-4610.2010.01774.x (2011).
21. Tietjen, G. E. et al. Recalled maltreatment, migraine, and tension-type headache: Results of the AMPP study. *Neurology* **84**, 132–140. https://doi.org/10.1212/wnl.0000000000001120 (2015).
22. Valfrè, W., Rainero, I., Bergui, M. & Pinessi, L. Voxel-based morphometry reveals gray matter abnormalities in migraine. *Headache* **48**, 109–117. https://doi.org/10.1111/j.1526-4610.2007.00723.x (2008).
23. Xue, T. et al. Intrinsic brain network abnormalities in migraines without aura revealed in resting-state fMRI. *PLoS One.* **7**, e52927. https://doi.org/10.1371/journal.pone.0052927 (2012).
24. Ma, M. et al. Exploration of intrinsic brain activity in migraine with and without comorbid depression. *J. Headache Pain* **19**, 48. https://doi.org/10.1186/s10194-018-0876-9 (2018).
25. Shan, X. et al. Shared and distinct homotopic connectivity changes in melancholic and non-melancholic depression. *J. Affect. Disord.* **287**, 268–275. https://doi.org/10.1016/j.jad.2021.03.038 (2021).
26. Steardo, L. Jr. et al. Application of support vector machine on fMRI data as biomarkers in schizophrenia diagnosis: A systematic review. *Front. Psychiatry* **11**, 588. https://doi.org/10.3389/fpsyt.2020.00588 (2020).
27. Zhang, C. et al. Disrupted interhemispheric coordination of sensory-motor networks and Insula in major depressive disorder. *Front. Neurosci.* **17**, 1135337. https://doi.org/10.3389/fnins.2023.1135337 (2023).
28. Regier, D. A., Kuhl, E. A. & Kupfer, D. J. The DSM-5: Classification and criteria changes. *World Psychiatry: Off. J. World Psychiatric Assoc. (WPA)* **12**, 92–98. https://doi.org/10.1002/wps.20050 (2013).
29. The International Classification of Headache Disorders, 3rd edition (beta version). *Cephalalgia: int. J. headache* **33**, 629–808. https://doi.org/10.1177/0333102413485658 (2013)
30. Chen, C. et al. Abnormal local activity and functional dysconnectivity in patients with schizophrenia having auditory verbal hallucinations. *Curr. Med. Sci.* **40**, 979–984. https://doi.org/10.1007/s11596-020-2271-4 (2020).
31. Tharwat, A. Parameter investigation of support vector machine classifier with kernel functions. *Knowl. Inf. Syst.* **61**, 1269–1302. https://doi.org/10.1007/s10115-019-01335-4 (2019).
32. Peng, Y. et al. A toolkit with friendly graphical user interface for multivariate pattern analysis of neuroimaging data. *Front. Neurosci.* **14**, 545. https://doi.org/10.3389/fnins.2020.00545 (2020).

33. Yang, Y. et al. Identifying functional brain abnormalities in migraine and depression comorbidity. *Quant. Imaging Med. Surg.* **12**, 2288–2302. https://doi.org/10.21037/qims-21-667 (2022).
34. Chandley, M. J. et al. Markers of elevated oxidative stress in oligodendrocytes captured from the brainstem and occipital cortex in major depressive disorder and suicide. *Prog. Neuro-psychopharmacol. Biol. Psychiatry*. **117**, 110559. https://doi.org/10.1016/j.pnpbp.2022.110559 (2022).
35. Friberg, T. R. & Borrero, G. Diminished perception of ambient light: A symptom of clinical depression? *J. Affect. Disord.* **61**, 113–118. https://doi.org/10.1016/s0165-0327(99)00194-9 (2000).
36. Golomb, J. D. et al. Enhanced visual motion perception in major depressive disorder. *J. Neurosci.* **29**, 9072–9077. https://doi.org/10.1523/jneurosci.1003-09.2009 (2009).
37. Zhang, X., Tang, Y., Zhu, Y., Li, Y. & Tong, S. Study of functional brain homogeneity in female patients with major depressive disorder. *Annual International Conference of the IEEE Engineering in Medicine and Biology Society. IEEE Engineering in Medicine and Biology Society. Annual International Conference* 2562–2565. https://doi.org/10.1109/embc.2016.7591253 (2016).
38. Sun, H. et al. Regional homogeneity and functional connectivity patterns in major depressive disorder, cognitive vulnerability to depression and healthy subjects. *J. Affect. Disord.* **235**, 229–235. https://doi.org/10.1016/j.jad.2018.04.061 (2018).
39. Yang, X. et al. Anatomical and functional brain abnormalities in unmedicated major depressive disorder. *Neuropsychiatr Dis. Treat.* **11**, 2415–2423. https://doi.org/10.2147/ndt.S93055 (2015).
40. Deng, Z. et al. The aberrant dynamic amplitude of low-frequency fluctuations in melancholic major depressive disorder with insomnia. *Front. Psychiatry* **13**, 958994. https://doi.org/10.3389/fpsyt.2022.958994 (2022).
41. Shen, Z. et al. Changes of grey matter volume in first-episode drug-naive adult major depressive disorder patients with different age-onset. *Neuroimage Clin.* **12**, 492–498. https://doi.org/10.1016/j.nicl.2016.08.016 (2016).
42. Zhang, B. et al. Altered functional connectivity density in major depressive disorder at rest. *Eur. Arch. Psychiatry Clin. NeuroSci.* **266**, 239–248. https://doi.org/10.1007/s00406-015-0614-0 (2016).
43. Vanni, S., Tanskanen, T., Seppä, M., Uutela, K. & Hari, R. Coinciding early activation of the human primary visual cortex and anteromedial cuneus. *Proc. Natl. Acad. Sci. U.S.A.* **98**, 2776–2780. https://doi.org/10.1073/pnas.041600898 (2001).
44. Calvert, G. A. Crossmodal processing in the human brain: insights from functional neuroimaging studies. *Cerebral cortex (New York, N.Y.)* **11**, 1110–1123. https://doi.org/10.1093/cercor/11.12.1110 (2001).
45. Yao, X. et al. Shared and distinct regional homogeneity changes in bipolar and unipolar depression. *Neurosci. Lett.* **673**, 28–32. https://doi.org/10.1016/j.neulet.2018.02.033 (2018).
46. Peterson, B. S. et al. Cortical thinning in persons at increased familial risk for major depression. *Proc. Natl. Acad. Sci. U.S.A.* **106**, 6273–6278. https://doi.org/10.1073/pnas.0805311106 (2009).
47. Du, Y. et al. Altered beta band spatial-temporal interactions during negative emotional processing in major depressive disorder: An MEG study. *J. Affect. Disord.* **338**, 254–261. https://doi.org/10.1016/j.jad.2023.06.001 (2023).
48. Price, D. D. Psychological and neural mechanisms of the affective dimension of pain. *Science* **288**, 1769–1772. https://doi.org/10.1126/science.288.5472.1769 (2000).
49. Parise, M. et al. Cuneus and fusiform cortices thickness is reduced in trigeminal neuralgia. *J. Headache Pain* **15**, 17. https://doi.org/10.1186/1129-2377-15-17 (2014).
50. Ter Minassian, A. et al. Dissociating anticipation from perception: Acute pain activates default mode network. *Hum. Brain. Mapp.* **34**, 2228–2243. https://doi.org/10.1002/hbm.22062 (2013).
51. Zhang, L. et al. Three major psychiatric disorders share specific dynamic alterations of intrinsic brain activity. *Schizophr Res.* **243**, 322–329. https://doi.org/10.1016/j.schres.2021.06.014 (2022).
52. Yang, M. et al. Disrupted olfactory functional connectivity in patients with late-life depression. *J. Affect. Disord.* **306**, 174–181. https://doi.org/10.1016/j.jad.2022.03.014 (2022).
53. Yi, S. et al. Neural activity changes in first-episode, drug-naïve patients with major depressive disorder after transcutaneous auricular vagus nerve stimulation treatment: A resting-state fMRI study. *Front. Neurosci.* **16**, 1018387. https://doi.org/10.3389/fnins.2022.1018387 (2022).
54. Broyd, S. J. et al. Default-mode brain dysfunction in mental disorders: A systematic review. *Neurosci. Biobehav. Rev.* **33**, 279–296. https://doi.org/10.1016/j.neubiorev.2008.09.002 (2009).

Acknowledgements
None.

Author contributions
W.C., C.Z.: Writing—original draft, Writing—review & editing, Methodology, Software. C.X.: Validation, Investigation, Resources. G.X., J.L.: Supervision, Project administration, Funding acquisition.

Funding
This study was supported by grants from the Guangdong Medical Science and Technology Research Fund Project (A2024206), the Guangdong Province Fund for Basic and Applied Basic Research (Grant No. 2023A1515140092).

Declarations

Competing interests
The authors declare no competing interests.

Ethical approval
This study involving human subjects was reviewed and approved by the Ethics Committee of the Third People's Hospital of Foshan (FSSY-LS202213), and informed consent was obtained from all participants.

Additional information
Correspondence and requests for materials should be addressed to J.L. or C.Z.